Surface radiation budget and role of clouds during the 2016 Study of the water VApour in the polar AtmosPhere (SVAAP) campaign at Thule, Greenland

Daniela Meloni[1], Tatiana Di Iorio[1], Alcide di Sarra[1], Antonio Iaccarino[1], Giandomenico Pace[1], Gabriele Mevi[2], Giovanni Muscari[2], Marco Cacciani[3], Julian Gröbner[4]

[1]Laboratory for Observations and Analyses of Earth and Climate, ENEA, Italy, e-mail: daniela.meloni@enea.it;
[2]Istituto Nazionale di Geofisica e Vulcanologia, Italy;
[3]Physics Department, University of Rome "La Sapienza", Italy;
[4]PMOD/WRC, Switzerland.

Abstract

The radiative balance of the Earth-atmosphere system is the driving motor of climate change, and polar regions are the most sensitive, at global level, to such changes [Serreze and Francis, 2006]. Among different factors, water vapour and clouds have the most important influence on surface radiative budget (SRB) in the polar regions, acting with complex feedback mechanisms [Curry et al., 1995; 1996]. For such reason there is an urgent need to investigate the cloud impact on the atmospheric radiative budget. The determination of cloud properties from satellite is problematic [Kato et al., 2006], thus requiring either long term measurements or intensive field campaigns.
The climate observatory at Thule (76.5° N, 68.8° W), Greenland, is devoted to climate change studies since 90's, with an international effort of different institutions: DMI, NCAR, ENEA, INGV, University of Rome (http://www.thuleatmos-it.it).
The Study of the water Vapour in the polar AtmosPhere (SVAAP) project, funded by the Italian Programme for Antarctic Research, is aimed at investigating the surface radiation budget, the variability of atmospheric water vapour, and the long-term variations in stratospheric composition and structure at Thule, in the framework of the international Network for Detection of Atmospheric Composition Change (NDACC). The SRB investigation is a common focus of both SVAAP and ARCA projects, the radiation balance being a key quantity in air-surface interaction.
In addition to continuing the long term measurements of stratospheric parameters, the project includes the realization of an intensive field campaign, which offered the possibility to study the cloud physical and optical properties and their impact on the surface radiative budget.
The field campaign was held from 5 to 28 July 2016. The instruments already operating at Thule observatory were: a lidar system for the stratospheric temperature profile (during nighttime) and of the tropospheric backscattering profile [di Sarra et al., 1998; di Sarra et al., 2002; Di Biagio et al., 2010], an Eppley PSP pyranometer and a Kipp&Zonen CGR4 pyrgeometer for the downward shortwave (SW) and longwave (LW) irradiance [Di Biagio et al., 2012], respectively, and the millimeter-wave spectrometer GBMS [Muscari et al., 2007; 2012] capable of measuring the stratospheric and mesospheric chemical composition.
New instruments for the SRB and for the characterization of the atmospheric state were installed for the campaign: an Eppley PSP pyranometer and a PIR pyrgeometer for the upward SW and LW irradiance, respectively; two Licor 190R sensors for the upwelling and downwelling photosynthetically active radiation (PAR); a Metcon actinometer for the downward actinc flux in the 280-700 nm spectral range; a modified CG3 pyrgeometer measuring downward irradiance in the 8-14 μm infrared window; a Hatpro microwave radiometer for the temperature and relative humidity tropospheric profiles, the integrated water vapour (IWV), and the liquid water path (LWP); VESPA-22 microwave spectrometer [Bertagnolio et al., 2012] for stratospheric water vapour profiles and IWV; a Heitronics infrared (9.6-11.5 μm) pyrometer for the sky brightness temperature (BT); a visible and an infrared sky cameras for the cloud cover; a meteorological

station. Moreover, 23 radiosonde were launched during the campaign to obtain vertical profiles of pressure, temperature, relative humidity, wind direction and speed up to about 30 km.

Data from the period 14-18 July are presented in this study. A specific algorithm was applied to the Hatpro measurements to retrieve the IWV in the high latitude conditions: the radiosonde IWV was compared to the Hatpro retrievals and the resulting absolute differences were below 5% (2 sigma). Figure 1 shows the time evolution of downward and upward SW irradiances, and the derived SW albedo. The first part of the campaign was characterized by stable cloud-free conditions, while alternation of cloudy and cloud-free sky occurred after 18 July (day number 200).

Figure 2 presents the time series of the sky infrared brightness temperature, the downward irradiance in the infrared window and in the broadband LW spectral range, and the upward LW irradiance. All the upward-looking instruments detect the atmospheric changes, although a larger variability is captured by the pyrometer due to its narrow field of view (about 1.5°). The small differences between the broadband and the infrared window irradiances are due to the small sensitivity to water vapour in the infrared window.

The cloud optical thickness (COT) can be derived following Barnard and Long [2004] from the downward SW irradiance and albedo, under the assumption of homogeneous cloud cover. The estimated COT is plotted in Figure 3. The cloud presence is associated with a decrease (increase) in SW (LW) irradiance, while changes depend on the cloud geometrical (base and top altitude), microphysical (phase, effective droplet radius, r_e, and their variation with altitude), and optical (COT, LWP, and their variation with altitude) properties.

Assuming that the liquid water content increases with altitude, the effective droplet radius can be retrieved. Figure 3 shows also the plot of the measured LWP, filtered for values lower than 0.4 kg m^{-2} [Löhnert and Crewell, 2003], and the derived values of r_e, which is generally below 20 μm. The distribution of the derived r_e (not shown) revealed peak values between 5 and 9 μm. It should be taken into account that this methodology is based on the use of measurements from different instruments, thus requiring a careful data selection.

The SRB can be computed from the SW and LW irradiance measurements, and is plotted in Figure 4. While the SW SRB is always positive during the measurement campaign, the LW SRB is negative under cloud-free conditions, becoming positive during cloud occurrence. The total (SW+LW) SRB is positive and its variability is dominated by the SW irradiance. Clouds reduce the SRB compared to the cloud-free periods, thanks to the dominating SW effect.

The availability of the cloud physical and optical properties and the atmospheric vertical profiles will allow to study in details the SW and LW cloud radiative effect by means of radiative transfer simulations.

References

Barnard, J. C, Long, C. N., 2004. A simple empirical equation to calculate cloud optical thickness using shortwave broadband measurements. J. Appl. Meteor., 43(7), 1057-1066.

Bertagnolio, P. P., Muscari, G., Baskaradas, J., 2012. Development of a 22 GHz groundbased spectrometer for middle atmospheric water vapour monitoring, Eur. J. Remote Sens., 45, 51-61, doi:10.5721/EuJRS20124506.

Curry, J. A., Schramm, J. L., Serreze, M. C., Ebert, E. E., 1995. Water vapor feedback over the Arctic Ocean. J. Geophys. Res., 100, 223–229.

Curry, J. A., Rossow, W. B., Randall, D., Schramm, J. L., 1996. Overview of Arctic Cloud and Radiation Characteristics. J. Climate, 9, 1731–1764.

Di Biagio, C., Muscari, G., di Sarra, A., de Zafra, R. L., Eriksen, P., Fiocco, G., Fiorucci, I., Fuà, D., 2010. Evolution of temperature, O_3, CO, and N_2O profiles during the exceptional 2009 Arctic major stratospheric warming as observed by lidar and millimeter-wave spectroscopy at Thle (76.5°N, 68.8°W), Greenland. J. Geophys. Res., 115, D24315.

Di Biagio C., di Sarra, A., Eriksen, P., Ascanius, S. E., Muscari, G., Holben, B., 2012. Effect of surface albedo, water vapour, and atmospheric aerosols on the cloud-free shortwave radiative budget in the Arctic. Climate Dyn., 39, 953-969.

di Sarra A., Bernardini, L., Cacciani, M., Fiocco, G., Fuà, D.1998. Stratospheric aerosols observed by lidar over northern Greenland in the aftermath of the Pinatubo eruption. J. Geophys. Res., 103, doi:10.1029/98JD00901.

di Sarra, A., Cacciani, M., Fiocco, G., Fuà, G., Jørgensen, T. S., 2002. Lidar observations of polar stratospheric clouds over northern Greenland in the period 1990–1997. J. Geophys. Res., 107(D12), 4152, doi:10.1029/2001JD001074.

Kato, S., Loeb, N. G., Minnis, P., Francis, J. A., Charlock, T. P., Rutan, D. A., Clothiaux, E. E., Sun-Mack, S., 2006. Seasonal and interannual variations of top-of-atmosphere irradiance and cloud cover over polar regions derived from the CERES data set,Geophys. Res. Lett., 33, doi:10.1029/2006GL026685.

Löhnert, U., Crewell, S., 2003. Accuracy of cloud liquid water path from ground-based microwave radiometry, 1, Dependency on cloud model statistics. Radio Sci., 38(3), 8041, doi:10.1029/2002RS002654.

Muscari, G., di Sarra, A. G., de Zafra, R. L., Lucci, F., Baordo, F., Angelini, F., Fiocco, G., 2007. Middle atmospheric O_3, CO_2, N_2O, HNO_3, and temperature profiles during the Arctic winter 2001–2002. J. Geophys. Res., 112, doi:10.1029/2006JD007849.

Muscari G., Cesaroni, C., Fiorucci, I., Smith, A. K., Froidevaux, L., Mlynczak, M. G., 2012. Strato-mesospheric ozone measurements using ground-based millimeter-wave spectroscopy at Thule, Greenland. J. Geophys. Res., 117, doi:10.1029/2011JD016863.

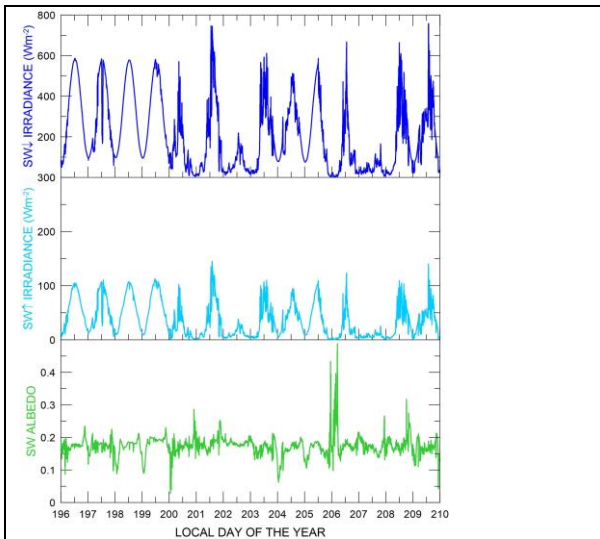Serreze, M. C., Francis, J. A., 2006. The Arctic amplification debate. Climatic Change, 76, 241-264.

Figure 1: *From top to bottom: time series of downward and upward SW irradiance, and derived surface albedo.*
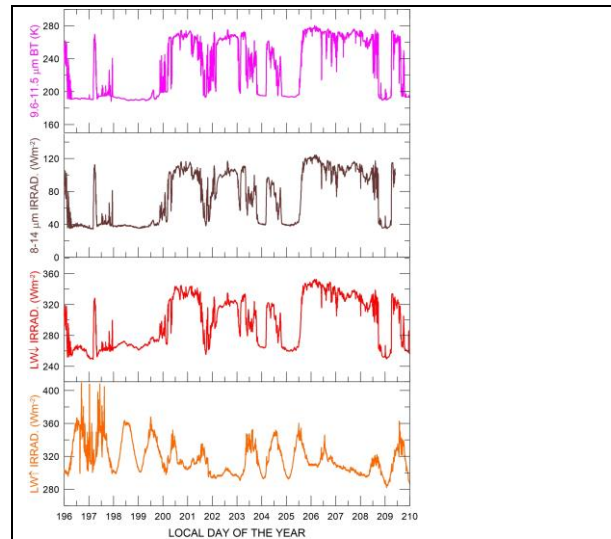

Figure 2: *From top to bottom: time series of window BT, downward infrared window and broadband LW irradiance, and upward LW irradiance.*
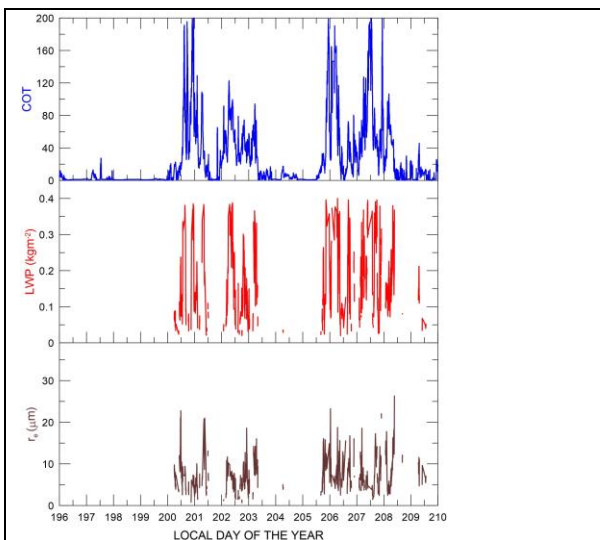

Figure 3: *From top to bottom: time series of COT, LWP and r_e.*
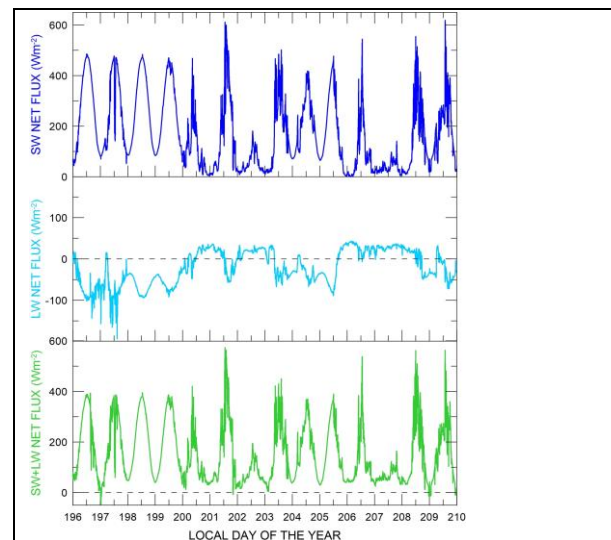

Figure 4: *From top to bottom: time series of the SW, LW and total (SW+LW) surface net fluxes.*